JOURNAL OF MODERN OPTICS, 1990, VOL. 37, NO. 4, 613–626

All-optical switching in a nonlinear resonator

G. S. McDONALD and W. J. FIRTH
Department of Physics and Applied Physics,
Strathclyde University, Glasgow G4 0NG, Scotland

Abstract. In this paper we consider some features of all-optical switching in a unidirectional ring cavity which is partially filled with a fast and saturably nonlinear medium. A comparative study of cross-talk for both signs of nonlinearity, in a two pixel (whole-beam switching) configuration, is made. A particular interaction modulation is discovered for two beams in the self-defocusing case. For self-focusing media, results are extended by consideration of large (part-beam switched) solitary arrays. Prescribed binary patterns may be stably encoded in a *single* cavity transit which is in sharp contrast to the hundreds of transits required for spontaneous stabilisation. These patterns are seen to be stable over thousands of transits.

1. Introduction

Our research is part of a global initiative to tackle a profound leap from the oversimplified, but instructive, plane wave analyses of nonlinear optical phenomenon to the real world of (finite width) optical beams making accumulative nonlinear interactions with matter. Recent research concerning all-optical switching has mainly involved the Kerr effects in nonlinear interferometers (NLI) and in nonlinear couplers (NLC). Switching of soliton-like pulses in both the NLI and NLC has only very recently been considered [1–5]. In these cases low energy, high contrast and stable switching have suggested solitons as the natural 'bits' for optical information processing. Here we shall investigate the suitability of 'bistable' spatial solitary waves as pixels in a transverse binary array.

2. Theory

In this work we closely follow the scheme and notation of Moloney and co-workers [6]. The complex field, $G_n(x, z)$, during its nth transit through our medium may be described by a nonlinear Schrödinger-type evolution equation:

$$2i\frac{\partial G_n}{\partial z}+\frac{\gamma}{p}\frac{\partial^2 G_n}{\partial x^2}+N(|G_n|^2)G_n=0. \tag{1}$$

We have concentrated on the planar waveguide case where the diffraction Laplacian reduces to an operator in one Cartesian dimension. The cavity boundary conditions complete a full transverse, and indeed infinite-dimensional, generalization of that considered by Ikeda [7]

$$G_{n+1}(x, 0)=A(x)+R\exp(i\Phi_0)\,G_n(x, p). \tag{2}$$

We shall make the assumption that the pump field, denoted $A(x)$, is detuned at least by a few homogeneous linewidths from the two-level atom resonance. Our nonlinearity is therefore dispersive in nature, $N(|G_n|^2)=-1/(1+2|G_n|^2)$. The scaling

0950–0340/90 $3·00

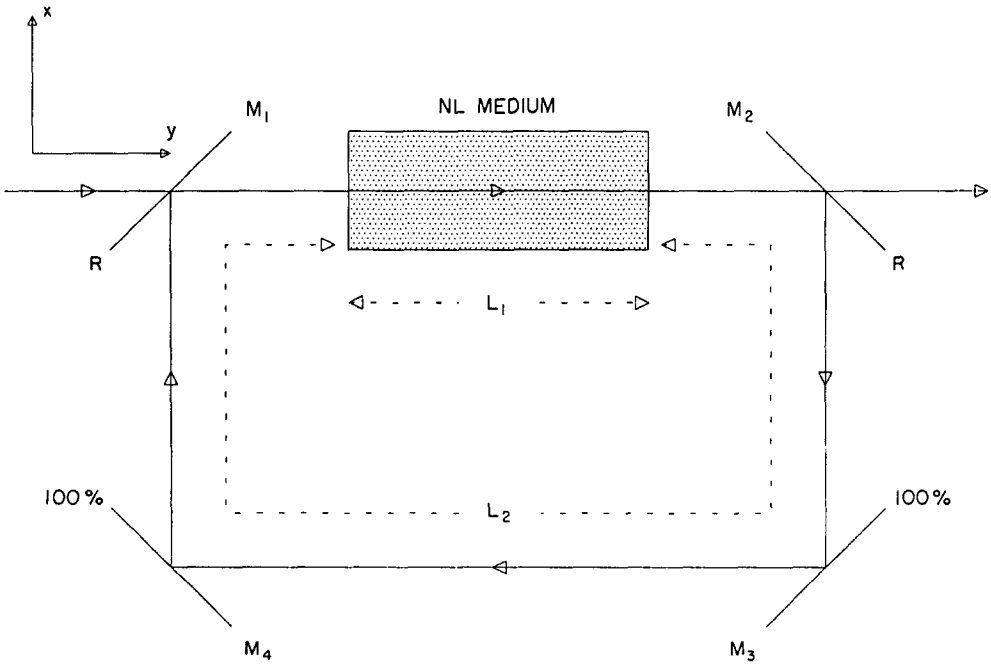

Figure 1. Our optical resonator, partially filled ($L_R=0{\cdot}3$) with a nonlinear medium. The laser beam enters through M_1 which, like M_2, has an intensity reflectivity of $R=0{\cdot}9$. Output through M_2 is monitored.

of the propagation and transverse dimensions (see figure 1) are such that we deal with an effective medium length, $p=\alpha_0 L_1/\Delta$, and our (beam) Fresnel number, F, is scaled into $\gamma=\ln 2/(4\pi F)$. Cavity parameters Φ_0, Δ and α_0 are the (scaled) mistuning, detuning and linear absorption coefficients respectively.

We normally allow for the medium to fill only part of the cavity; performing linear lossless propagation in the remainder. In the simulations presented an integration is firstly performed to the output mirror, M_2, to allow data collection before completing the resonator circuit. In all cases $p=2\eta$ and $\Phi_0=0{\cdot}4\eta$, where $\eta=\pm 1$ for self-focusing and self-defocusing media respectively. Integrations within the medium are performed using the efficient split-step Fourier operator method [8].

To effect memory we may need to spatially modulate the medium or the input light or both. Medium pixellation leads to rather involved considerations, as can be illustrated by particular examples cited from the physics of nonlinear interference filters, where both analytic [9] and experimental [10] work has been performed. In the light of this, we shall examine pixellation through spatial modulation of *only* the pump field. Our work therefore broadly follows on from publications which dealt with bistable arrays induced in a nonlinear Fabry–Perot [11]. Those studies modelled the specific physics of InSb etalons where diffusive coupling has been seen to be the dominant transverse effect [12]. Here we shall study the case of dominantly diffractive coupling and seek to establish device prospects and limitations for this kind of interpixel cross-talk.

Neglecting diffraction allows much analytic progress to be made, whereas its inclusion results in a relatively intractable system for which full numerical simulations are necessary. It is hoped that, in the self-focusing case, the attracting nonlinear basis (solitary waves) will simplify the spatial complexity to consideration of only these (natural) nonlinear cavity modes. Drawing an analogy between diffusion length and an equivalent 'diffraction length', we may expect coupling to be essentially short-ranged (nearest-neighbour) as in the diffusive case [11, 13]. This argument is strengthened if we recall the exponential decay of interaction force, with separation, found for exact soliton solutions of the nonlinear Schrödinger equation [14]. The case of longer-ranged interaction forces arise in thermal cross-talk, such as in nonlinear interference filters [15], and is manifest through a '$1/r$' dependence of interpixel coupling constants.

Nearest-neighbour interaction allows for a preliminary study of two-beam coupling. Such a study has already been performed on a similar system considering a single low Fresnel number [16]. Here we present results from a two-beam coupling investigation for *both* signs of nonlinearity and in a model which neglects saturable absorption, which generalizes that work and provides necessary underpinning for our array studies.

3. Results and discussion

3.1. *Two-beam coupling*

For parallel operation of two all-optical switches on the same etalon, we choose to work with a low Fresnel number ($F=1$) and hence within the whole-beam switching regime [17]. The chosen form of $A(x, t)$ in this case is

$$A(x,t)=a_{01}\exp[-(x-x_1)^2]+a_{02}(t)\exp[-(x+x_1)^2+\mathrm{i}\Delta\Phi]. \tag{3}$$

Our hold beam separation will be referenced in units of intensity f.w.h.m. so we define $\mathrm{X0}=[(2/\ln 2)]^{1/2}x_1$. Temporally, both beams are held at a working point, a_{H}, while $a_{02}(t)$ encompasses an additional square pulse, of amplitude $a_{\mathrm{S}}-a_{\mathrm{H}}$, on the left beam. These amplitudes are parameterized around the peak input amplitudes of up- and down-switching ($a\wedge$ and $a\vee$ respectively) and are taken as

$$\begin{aligned} a_{\mathrm{H}}&=a\vee+c_{\mathrm{H}}(a\wedge-a\vee),\\ a_{\mathrm{S}}&=c_{\mathrm{S}}a_{\mathrm{H}}. \end{aligned} \tag{4}$$

In this system, $c_{\mathrm{H}}=0{\cdot}75$ and $c_{\mathrm{S}}=1{\cdot}5$ supply safe hold points, free from overshoot and undershoot switching, and modest amplitude and necessary duration of address. An overall phase difference, $\Delta\Phi$, between the pump fields is also included. Such a factor may arise, for example, due to beam *multiplexing*. The key problem is determining under what values of separation and relative phase of the pumps the left-hand beam can be independently switched.

Figure 2 gives examples from simulations in the self-focusing case. The dashed curve is the prescribed hold beams whereas the resonator output profiles prior to, during, and after the address are drawn bold. For $\mathrm{X0}=2{\cdot}0$ and $\Delta\Phi=0{\cdot}0$, part (*a*), switching of the left-hand beam also triggers the right-hand beam, after which they are in phase with each other and have coalesced in the final plot. However, for $\mathrm{X0}=2{\cdot}25$ the left-hand side can be selectively addressed. In this case a slight drop in amplitude of the right-hand beam occurs due to the finite amount of cross-talk from the 'on' beam which has made a phase transition to the upper branch of

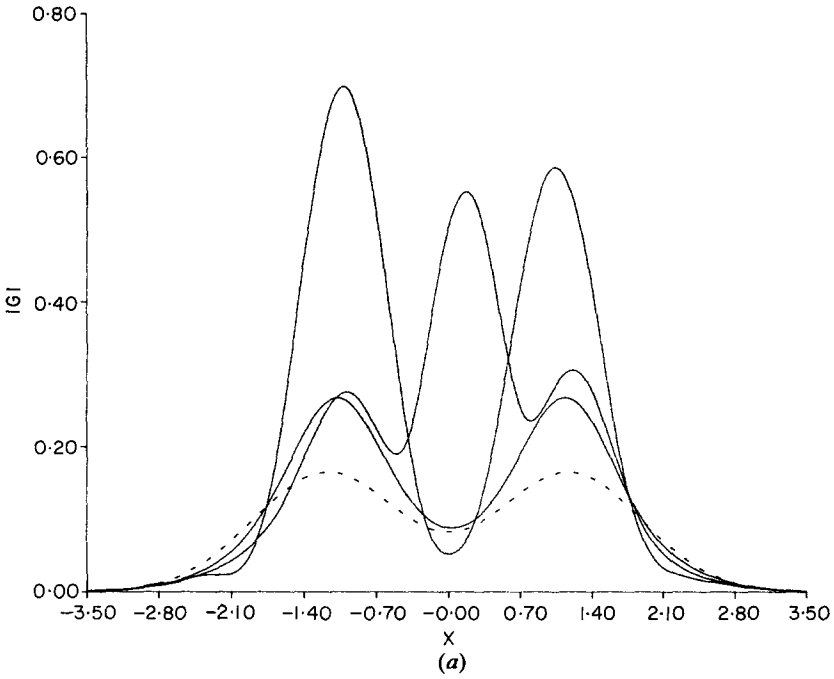

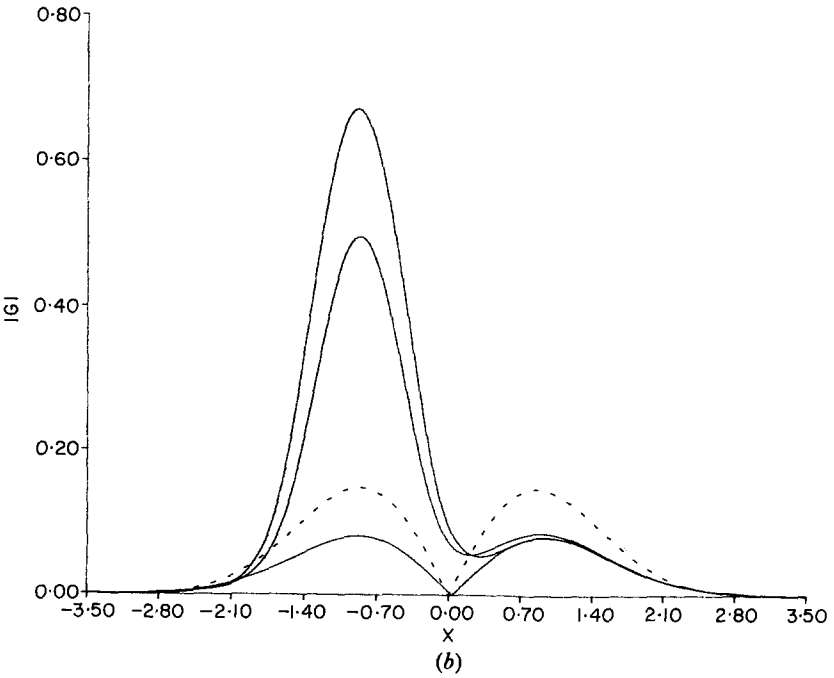

Figure 2. $\eta = +1$. Spatial profiles before, during and after the left beam has been addressed. In part (*a*) a f.w.h.m. (intensity) separation of hold beams, X0 = 2·0, is insufficient to maintain independent switching. In (*b*) pixel independence at X0 = 1·25 is achieved by application of an overall phase differential ($\Delta\Phi = \pi$) to the pump fields.

approximately π rad. When $\Delta\Phi=\pi$, part (*b*), relative beam phase again causes a degree of annihilation, this time reducing the peak beam amplitude prior to switching. This restraint, in conjunction with the intermediate destructive phase barrier, halts the switching wave allowing independent switching down to an impressive X0 = 1·25. When X0 is increased, the initial mutual annihilation is mostly confined to between the beams and this alone is sufficient to inhibit induced switching. This indicates that it is not just excessive cross-talk that prevents cross-switching when X0 is very low.

Performing the corresponding experiments for the self-defocusing nonlinearity produces much less encouraging results. There is one slight difference in switching strategy here, in that the pump fields are ramped into place. This is done well before the switch is implemented and is a prudent precaution in view of the much reduced input amplitude range for bistability.

Spatial profiles elucidating evolution during address are shown for the parameter set X0 = 4·0, $\Delta\Phi$ = 0·0 in figure 3 (*a*). Rapid oscillations can be seen growing on the broad exponential wings and, at certain stages in the switch period, it is hard to distinguish them from the unswitched beam. It is around this value of X0 where the right-hand beam becomes discernible after the switch has been removed, and, in this sense, could be compared to the self-focusing minimum of 2·25. Problems of poor switch contrast are also quite apparent. The most unstable modulational wavelength, in terms of the plane wave instability [18], is on the scale of the beam separation—this is indicated by the confinement of the left-hand beam just as it starts

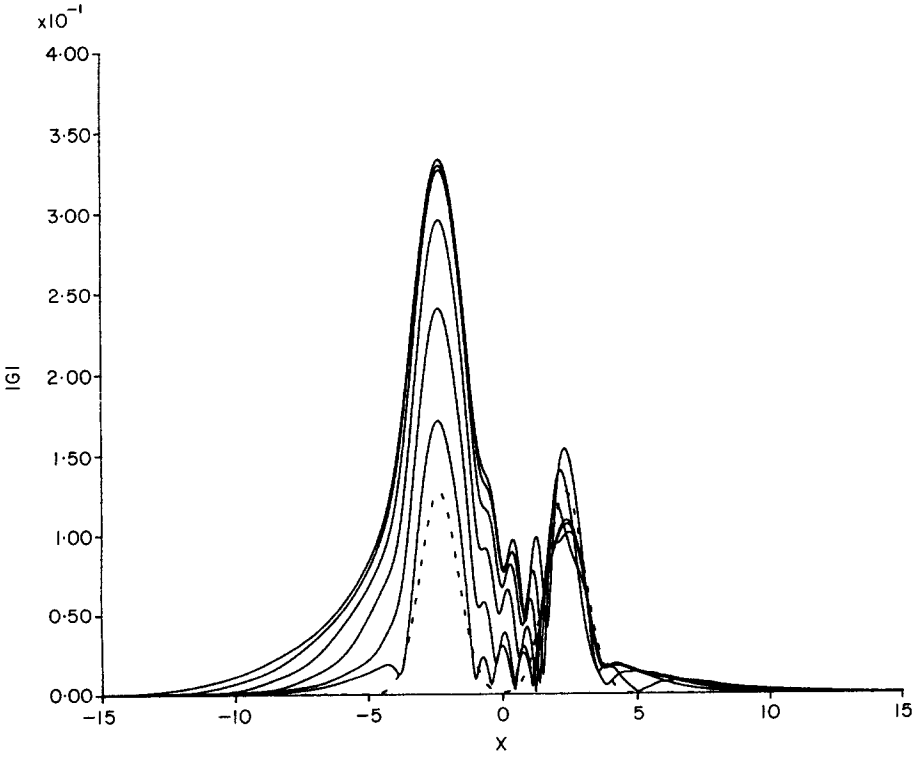

Figure 3 (*a*)

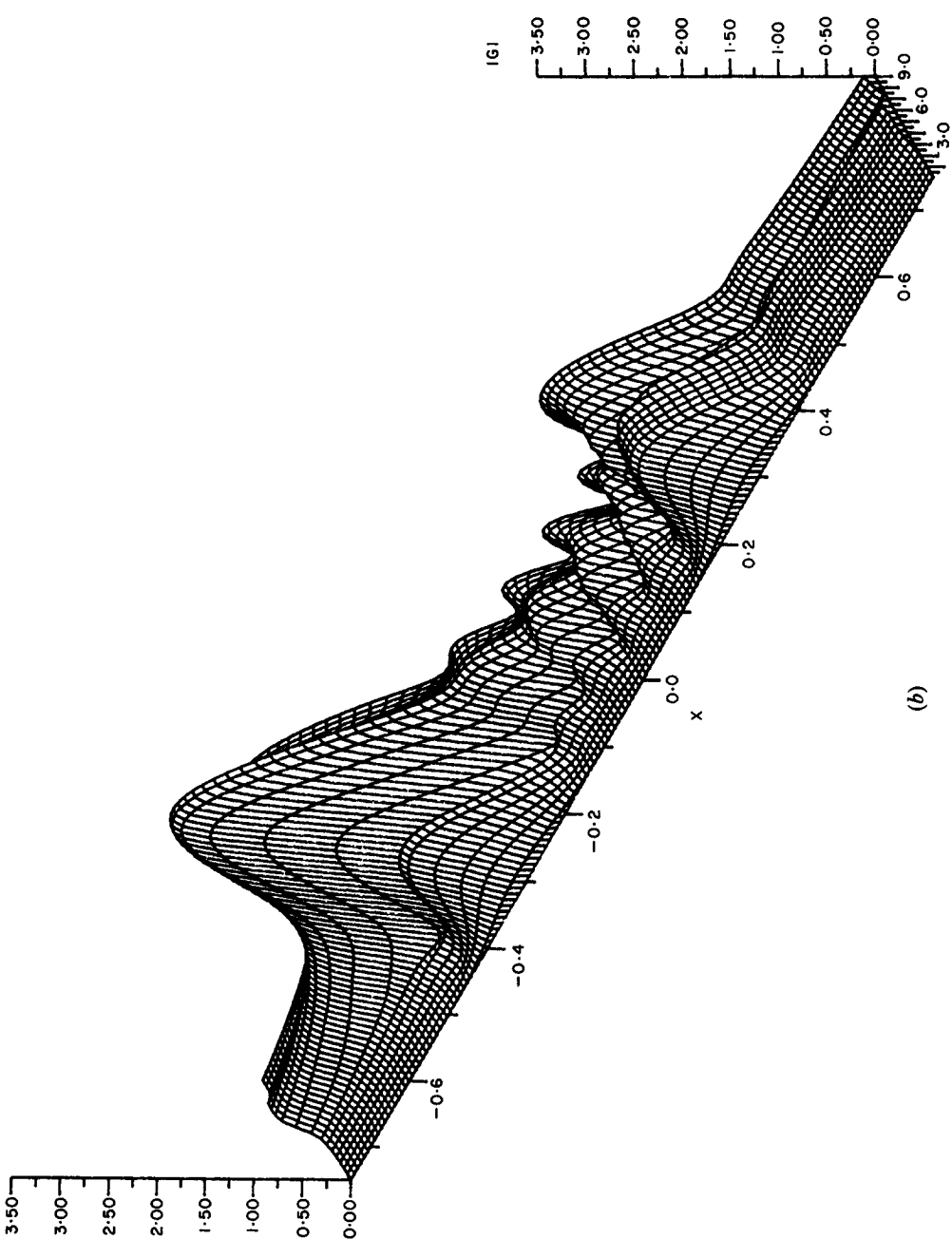

Figure 3. $\eta = -1$. Part (*a*) shows output during implementation of address when $X0 = 4{\cdot}0$ and $\Delta\Phi = 0{\cdot}0$. In (*b*) hold beam initialization, switching and subsequent evolution are shown for $X0 = 5{\cdot}0$, $\Delta\Phi = \pi$.

to switch. In view of this, and because this new modulation only occurs *between* the two beams, it is immediately obvious that it is due solely to beam interaction or nonlinearly trapped (standing) radiation modes.

One may expect that the relative phase of the beams could have a strong effect on the spatial interaction pattern, but it has been found that significant qualitative differences only occur when $X0 \leqslant 3{\cdot}0$. Figure 3 (*b*) shows the full temporal sequence when $X0 = 5{\cdot}0$, $\Delta\Phi = \pi$. Modulations remain strong in this simulation and the spatial displacement of the right beam, as it becomes strongly modulated *into* the pattern (also present for $\Delta\Phi = 0{\cdot}0$), is quite evident. At lower separations, and $\Delta\Phi = 0{\cdot}0$, beams quickly merge during the address producing a singularly broad, and ultimately spatially symmetric, transmitted beam whereas for $\Delta\Phi = \pi$ output beams retain both phase character and resolution through an annihilation trough. Neither case permits recovery of the address information through (reasonably sensitive) intensity discriminators although address history *is* embedded into the system in the form of a small (nonlinear) spatial shift of the beams.

The interaction modulation has been seen to have a wavelength that grows slightly when the beams are close together and falls to an approximately constant value at larger separations. Also note that the whole pattern shifts across the transverse domain quickly adjusting to changes in the amplitude of the left-hand beam.

To explain the nature of these modulations, the particular case $X0 = 7{\cdot}0$, $\Delta\Phi = 0{\cdot}0$ is taken, see figure 4 (*a*). Here interbeam oscillations are numerous and, by virtue of the large separation chosen, the interaction modulation extending beyond the right-hand peak is slight. For this case, we have (approximately) reconstructed the individual complex field profiles, that each beam would have alone, using the outer wings as data. Then, by superimposition of these, we have obtained a pattern strikingly similar to the original data, as can be seen in figure 4 (*b*). The origin of this effect is thus not, in itself, an accumulative process of evolution but is a strong interference pattern.

The slight differences, between figures 4 (*a*) and (*b*), may be attributed to spatial discretisation, finite cross-talk which extended over the right peak and also to the evolution of this interference pattern during intermediate cavity transits. When the smooth profile section of the switched beam is plotted on the complex field plane, figure 5 (*a*), we see that the field vector spirals down to the origin and also that saturation of the nonlinearity in the beam peak slows down the *runaway phase delay*. These phase profiles, caused by the additive effect of diffraction and sign of nonlinearity, are in stark contrast to those in the self-focusing case (not shown) where phase gradients balance and stabilise. The spatial frequency of the phase oscillations is displayed in figure 5 (*b*) on which profile locations where the Argand trajectory passes through the real axis are marked. Such representations allow the inter-beam structure to be immediately inferred, explaining why close beams produce larger wavelength patterns and showing that the interaction wavelength should become nearly constant for larger separations. The effect of an overall phase difference between the beams can also be explained as one now expects only a spatial shift in the pattern, of at most one modulation wavelength.

3.2. *Optical solitary wave memory arrays*

The spontaneous occurrence of spatial solitary waves in our system has already been predicted by both numeric and analytic studies [6, 19]. An example of

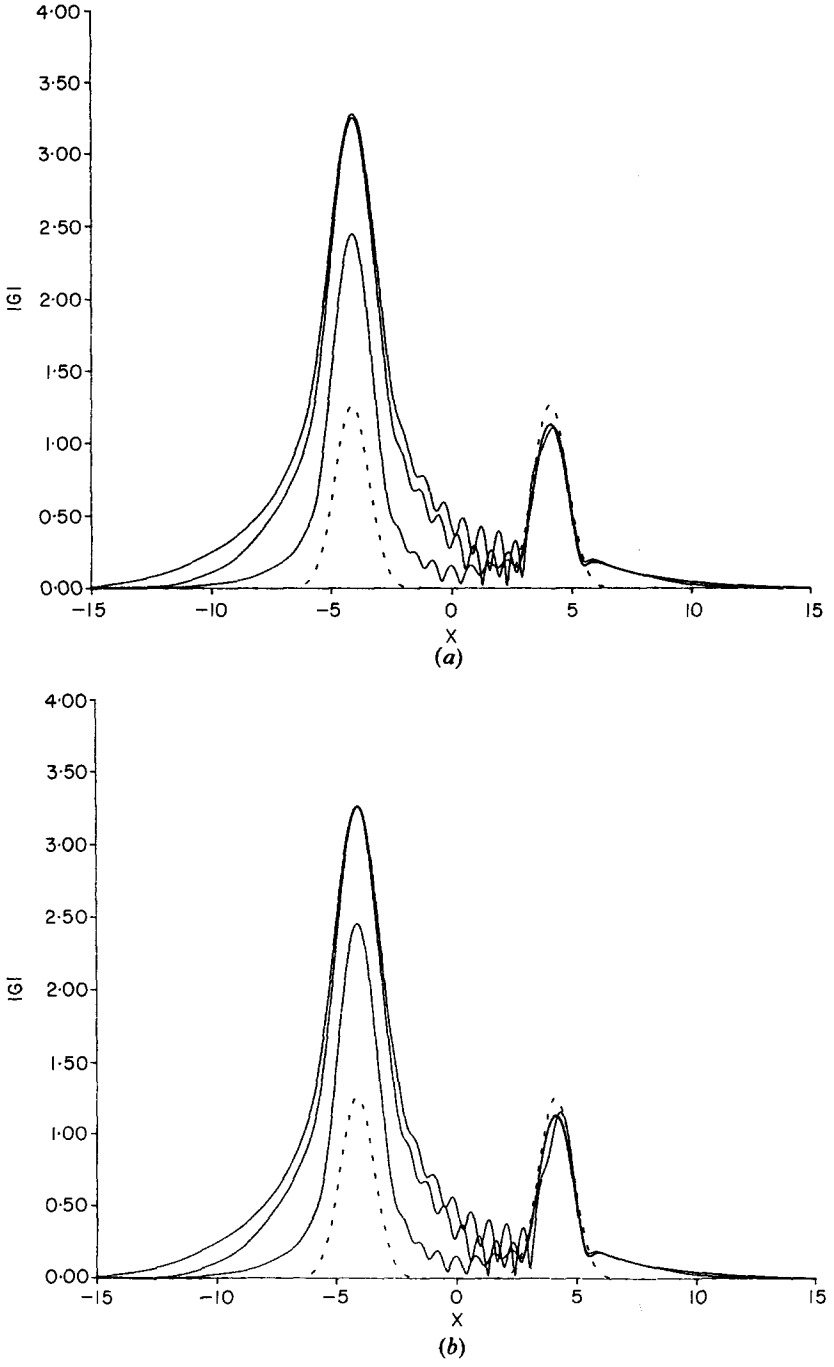

Figure 4. $\eta = -1$. Part (*a*) shows actual resonator output during switching for X0 = 7·0, $\Delta\Phi = 0{\cdot}0$ while (*b*) is the reconstruction using only the outer wings of each beam as data (see text for details).

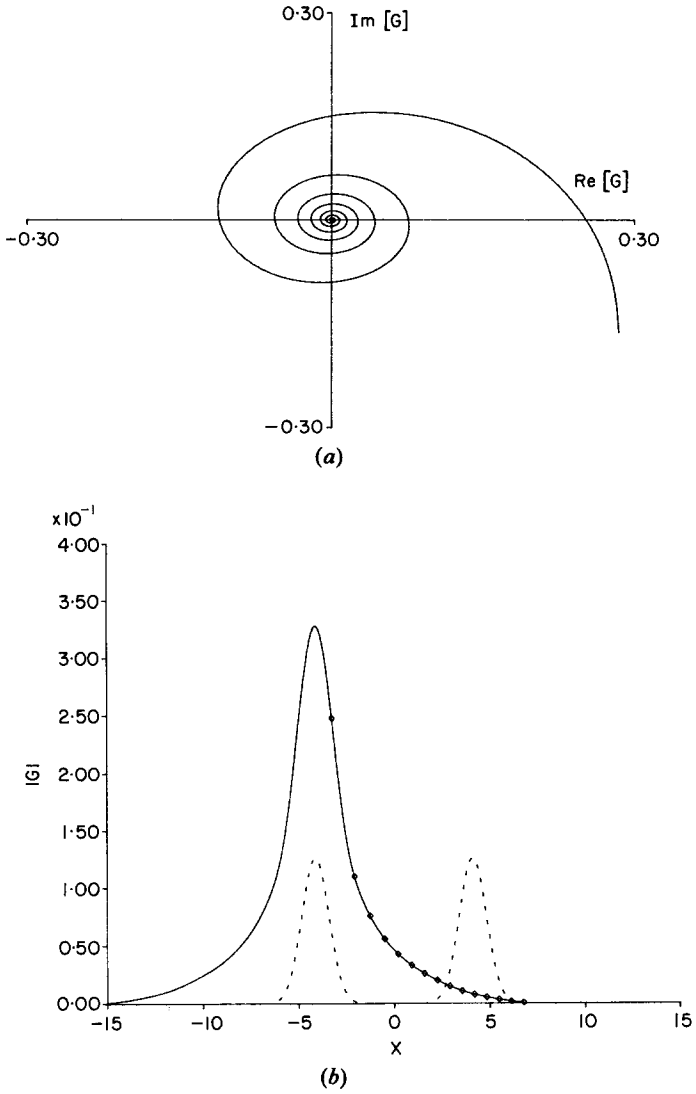

Figure 5. In (*a*) the smooth exponential wing of the switched beam, at the end of the address shown in figure 4, is plotted in the Argand plane. For (*b*) the reconstructed beam is shown and points where the Argand trajectory passes through the real axis are marked.

spontaneous organisation of a broad ($F=50$) beam into a stationary pattern of three solitary waves is given in figure 6. Note that over 100 cavity transits are required for stabilisation. Now we examine the feasibility of *inducing* these robust attractors on broad beams ($F\gg1$) by means of external (part-beam) address. Our exploration is towards effecting a parallel binary memory array by quickly encoding the address pattern on to the circulating beams asymptotic solitary basis [6]. We shall deal with the self-focusing sign of nonlinearity and pursue pixel site definition by hold beam modulation. To this end, our hold beam is a sinusoidally modulated

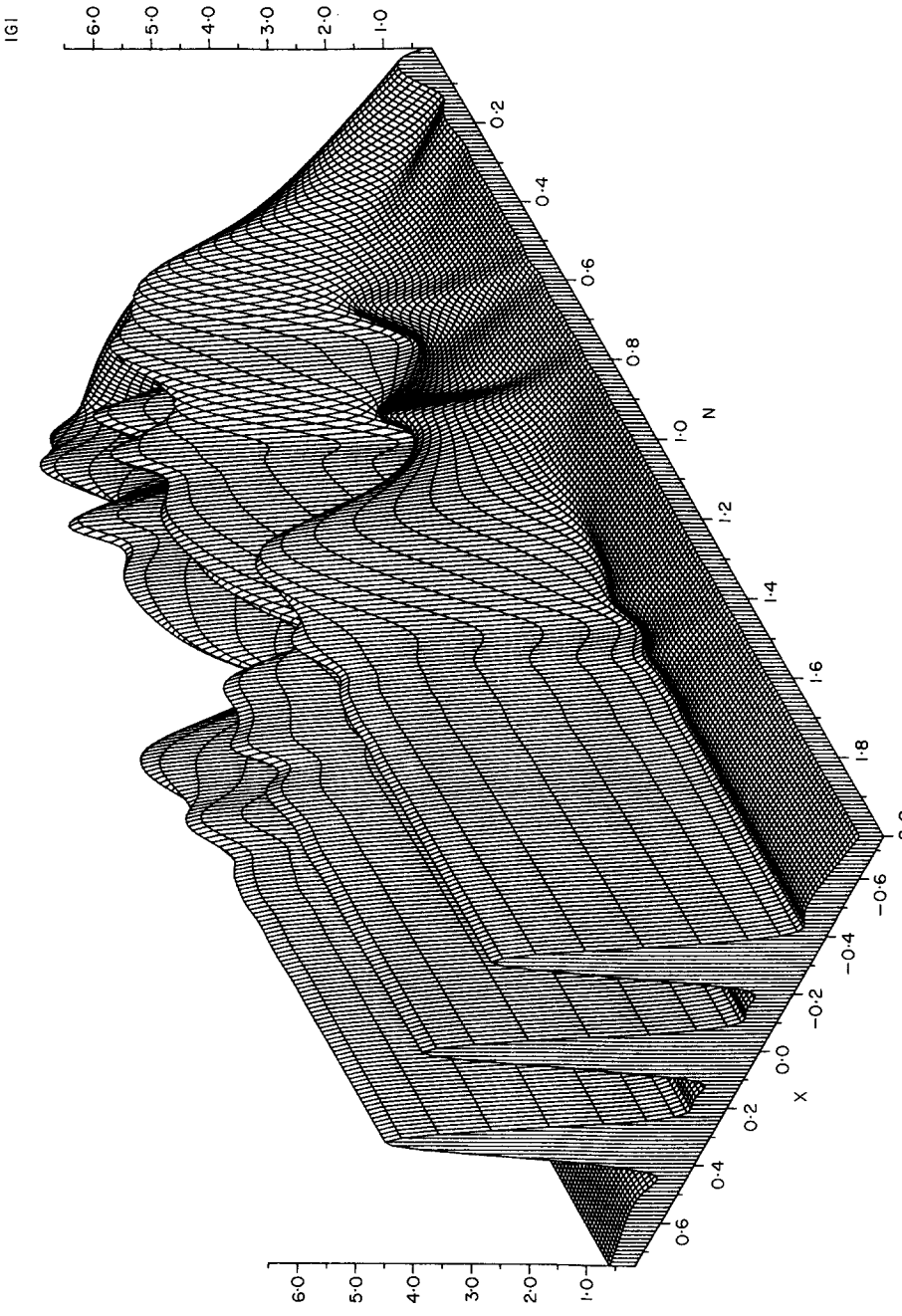

Figure 6. Spontaneous organisation of a stationary pattern of three solitary waves from a broad ($F=50$) Gaussian beam, as discovered by J. V. Moloney *et al.* N is in units of 100 cavity transits.

Gaussian (5). Such a beam may be easily produced experimentally by interference techniques.

$$A(x) = A_0 [1 + M \cos (k_m x)] \exp (-x^2). \tag{5}$$

The modulation depth is given by $M (|M| \leqslant 1)$ which may assume either sign depending on whether a finite odd or even number of pixel sites is desired. The density of the transverse array scales with the spatial pixellation frequency, k_m. The most obvious initial constraint on array size is the requirement that pixel locations must be such that the local hold beam amplitude lies between the appropriate bistable switch points, denoted A_{up} and A_{down} in figure 7. These switch levels are higher than those calculated for the smooth beam, as finite M entails additional intensity gradients, and their determination necessitated a preliminary switching study not only on the full set $\{A_0, M, k_m\}$ but, also, considering address characteristics. A_0 and peak (Gaussian) address amplitude, A_S, are parameterized, in a similar manner to the two beam case, as

$$A_0 = A_{down} + C_H (A_{up} - A_{down}), \qquad A_S = C_S A_0. \tag{6}$$

To avoid overshoot and critical slowing down, the global maximum of the hold beam is chosen to be approximately 70% into the working range, requiring $C_H \leqslant 0{\cdot}7$. Also shown in figure 7 are the address Gaussians, in the configuration '1101001110101110101'. It is now clear that the address beams need to be sufficiently well resolved to avoid induced switching in adjacent sites and, with hindsight, we shall present results here for which X0 is kept fixed at 4·0. This allows us to concern ourselves only with switch amplitude, where, at any F, (scaled) switch power is given by A_S^2 and switch energy is proportional to the product $A_S^2 T$, where T

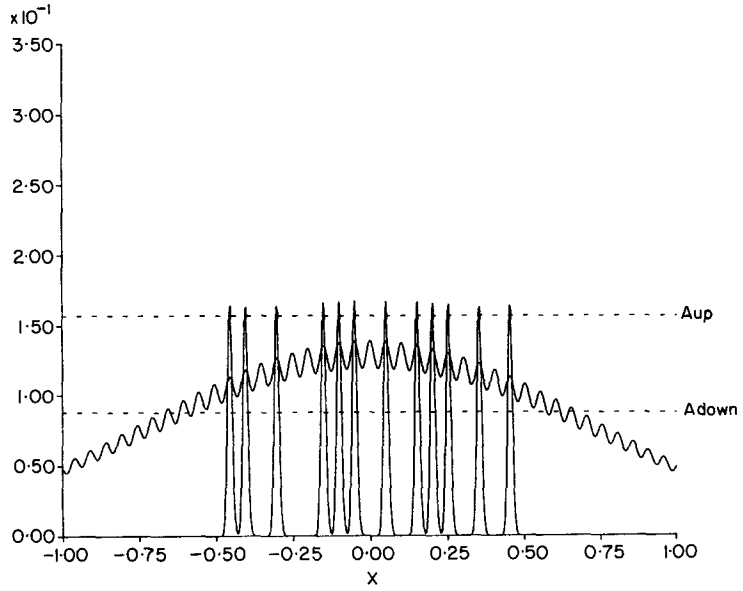

Figure 7. Our sinusoidally modulated hold beam with respect to the appropriate up- and down-switching amplitudes. Encoding of binary patterns on the circulating beam is attained by temporally abrupt superimposition of the addressing Gaussians.

is the duration of the temporally square address (in units of cavity transit time). The choice of C_S depends strongly on that of T as there is a distinct trade-off between switch power and duration. The subtleties of this and other scalings, involving the temporal switching dynamics, have been the subject of an extensive study [20].

Differences between spontaneous stabilisation and the part-beam switched arrays needs to be clarified at this point. Firstly, in the spontaneous case, the pixel count seems to depend upon how many full solitary widths, in groups of 1, 2 or 3, can fit into the switched-on region, each group being separated by a small lower branch node. The size of this on-region depends upon the peak amplitude of the pumping beam, which is quite evidently above the up-switching threshold. In part-beam switching, uniformity demands that there are lower branch nodes between each pixel and, by definition, the peak hold beam amplitude must lie *below* this switching point. Secondly, it has been found that the simple criterion of working between the two switch points is not sufficient and that marginally stable end pixels can disrupt the stability of the whole array [21]. Unaddressed end pixels seem to enable a bufferring of the array from the 'edge instabilities' and allow the hold beam modulation to effectively 'tile the box' in which the solitary waves sit.

In the following simulations the modulated hold beam is ramped into position during the first 20 round trips and then held at the operational point for a further 10 before the address is implemented. We present results for which a finite amount of spatial modulation ($M=0{\cdot}08$) is incorporated into our hold beam. Existence of index gradients arising from the lower branch pedestal and spatial solitary wave interaction forces have, to date, necessitated some form of 'pinning forces' [22]. Solitary wave switching on finite beams has been extended out to a nineteen-bit array for which $F=3565$ and $k_m=124{\cdot}4$ were used. To preserve numerical accuracy, any further extension would require a prohibitive leap in computational requirements. The importance of using such a large array prompts us to try selective simulations out to multiples of 1000 round trips. The adopted limit was 3000. In figure 8 the resonator

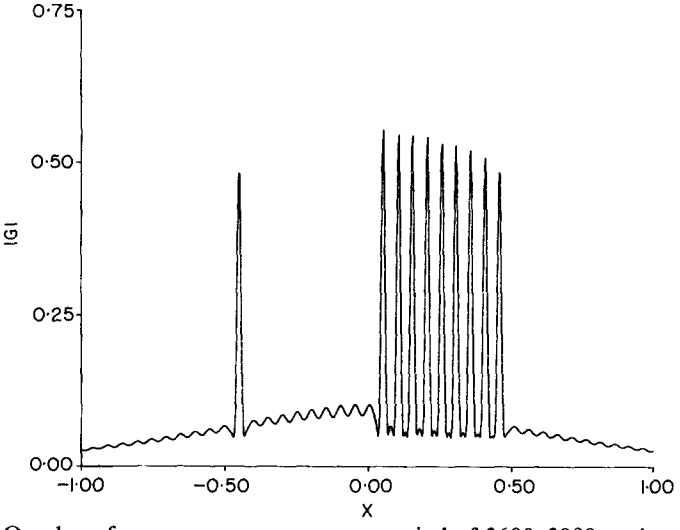

Figure 8. Overlay of resonator output over a period of 2600–3000 cavity transits. In this simulation the hold beam was allowed 30 transits for initialization and then a highly asymmetric '1000000000111111111' was encoded in the subsequent five transits.

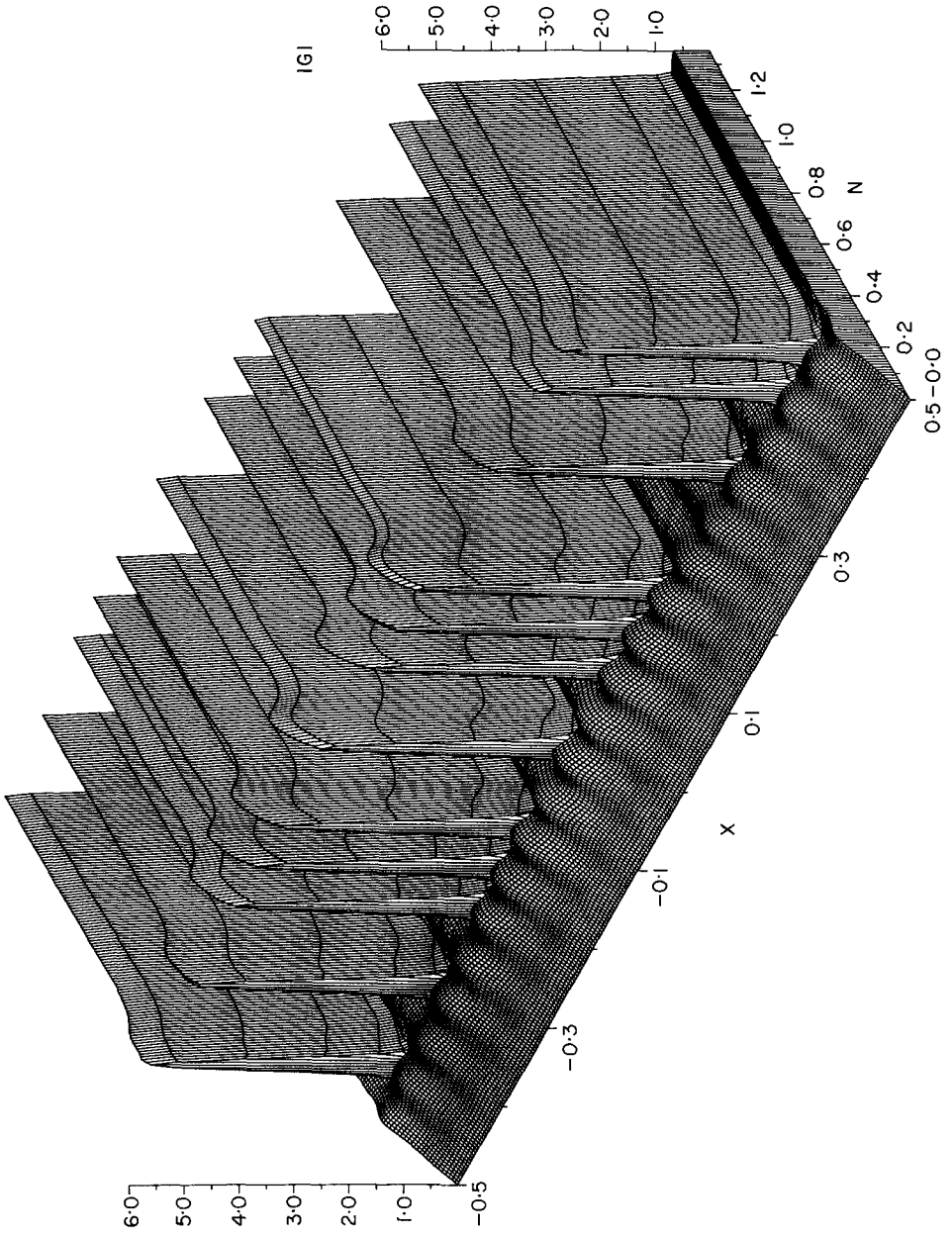

Figure 9. Hold beam initialization and subsequent address of a quasi-random 19-bit pattern in a single cavity transit. N is in units of 100 cavity transits.

output after a highly asymmetric encoding ('1000000000111111111') is presented in overlay format for the final 400 cavity transits. Figure 9 displays the address of a quasi-random pattern in a *single* cavity transit. Switch-on time has been seen to be a simple and controllable function of address specifications.

4. Summary

For parallel operation of two optical switches on the same etalon, it has been found that self-focusing media are highly favourable. For both signs of nonlinearity, separations necessary for independent switching have been determined. In the self-focusing case inclusion of a (possibly multiplexed) phase differential between the pump fields was found to enhance packing density. Poor contrast and, more importantly, a high degree of interpixel structure was found for the self-defocusing beams. At separations which were optimal for the positive sign of nonlinearity, an unswitched pixel becomes barely discernible from the cross-talk modulation due to the neighbouring 'on' pixel. This modulation was shown to arise from a spiralling phase profile which can be explained as due to an additive effect of nonlinearity and diffraction.

For part-beam switching, in the self-focusing case, it has been shown that the asymptotic solitary basis may be encoded with binary patterns in just a *single* cavity transit and that the circulating beam subsequently retains this information over thousands of round trips suggesting it as a strong candidate for nonlinear memory elements.

References

[1] Doran, N. J., and Wood, D., 1987, *J. opt. Soc. Am.* B, **4,** 1843.
[2] Doran, N. J., and Wood, D., 1988, *Optics Lett.*, **13,** 56.
[3] Blow, K. J., Doran, N. J., and Nayar, B. K., 1989, *Optics Lett.*, **14,** 754.
[4] Trillo, S., Wabnitz, S., Wright, E. M., and Stegeman, G. I., 1988, *Optics Lett.*, **13,** 672.
[5] Trillo, S., Wabnitz, S., Wright, E. M., and Stegeman, G. I., 1989, *Optics Commun.*, **70,** 166.
[6] Adachihara, H., McLaughlin, D. W., Moloney, J. V., and Newell, A. C., 1988, *J. math. Phys.*, **29,** 63.
[7] Ikeda, K., 1979, *Optics Commun.*, **30,** 257.
[8] Hardin, R. H., and Tappert, F. D., 1973, *SIAM Rev.*, **15,** 423.
[9] Abraham, E., Godsalve, C., and Wherrett, B. S., 1988, *J. Phys.*, **49,** 43.
[10] Kar, A. K., Harris, R. M., Buller, G. S., Smith, S. D., and Walker, A. C., 1988, *J. Phys.*, **49,** 443.
[11] Firth, W. J., and Galbraith, I., 1985, *IEEE J. quant. Electron.*, **21,** 1399.
[12] Hagan, D. J., Mackenzie, H. A., Al-Attar, H. A., and Firth, W. J., 1985, *Optics Lett.*, **10,** 187.
[13] Richardson, H., Abraham, E., and Firth, W. J., 1987, *Optics Commun.*, **63,** 199.
[14] Gordon, J. P., 1983, *Optics Lett.*, **8,** 596.
[15] Abraham, E., 1986, *Optics Lett.*, **11,** 689.
[16] Tai, K., Moloney, J. V., and Gibbs, H. M., 1982, *Optics Lett.*, **7,** 429.
[17] Moloney, J. V., and Gibbs, H. M., 1982, *Phys. Rev. Lett.*, **48,** 1607.
[18] McLaughlin, D. W., Moloney, J. V., and Newell, A. C., 1985, *Phys. Rev. Lett.*, **54,** 681.
[19] McLaughlin, D. W., Moloney, J. V., and Newell, A. C., 1983, *Phys. Rev. Lett.*, **51,** 75.
[20] McDonald, G. S., 1989, Ph.D. thesis, Strathclyde University.
[21] McDonald, G. S., and Firth, W. J., (to be published).
[22] McDonald, G. S., and Firth, W. J., 1990, *J. opt. Soc. Am.* B (submitted).